International Journal of Precision Engineering and Manufacturing-Green Technology (2020) 7:481–492
https://doi.org/10.1007/s40684-019-00031-6

Online ISSN 2198-0810
Print ISSN 2288-6206

REGULAR PAPER

Robust and Chemically Stable Superhydrophobic Aluminum-Alloy Surface with Enhanced Corrosion-Resistance Properties

Sumit Barthwal[1] · Si-Hyung Lim[2]

Received: 30 October 2018 / Revised: 1 January 2019 / Accepted: 11 January 2019 / Published online: 14 February 2019
© Korean Society for Precision Engineering 2019

Abstract

We report a simple method for fabricating micro-nanoscale structures consisting of irregular microscale plateaus with a self-assembled network of zinc oxide nanopetals on an aluminum alloy substrate. The method involves a combination of chemical etching with a hydrothermal process, followed by Polydimethylsiloxane coating via a simple vapor deposition method. Following the coating, surface displays superhydrophobicity with water contact angle of 161° and a sliding angle of 4°. The effect of morphological changes on wettability is examined by varying the hydrothermal processing time. The chemical stability of the superhydrophobic surfaces is examined in a wide range of corrosive media. After being immersed in a 3.5 wt% NaCl solution for 1 month, the surface retained its superhydrophobicity. The potentiodynamic polarization test results reveal that the superhydrophobic surface highly improves the corrosion resistance performance of the bare aluminum surface by three orders of magnitude. In addition, surface exhibited good mechanical durability against sandpaper abrasion, and long-term stability in the ambient environment. The proposed fabrication technique operating at relatively low temperature is simple and provides a new approach for production of large-scale three-dimensional superhydrophobic surfaces for various applications.

Keywords Superhydrophobic · Al alloy · ZnO · Micro-nano · Anti-corrosion · Durability

1 Introduction

Biomimetic superhydrophobic surfaces with a water contact angle (WCA) of greater than 150° and a sliding angle (WSA) of less than 10° have attracted significant attention within the industrial world as well as the scientific community. These artificial surfaces have a broad range of applications including examples such as self-cleaning [1, 2], anti-icing [3], oil/water separation [4], corrosion resistance [5, 6], drag reduction [7], and antifouling technologies [8]. A substantial number of studies have been carried out and it is now well documented that surface roughness (a combination of micro- and nanoscale structures) and surface energy (low-surface-energy materials) are the key parameters for developing artificial surfaces with superhydrophobic properties. Inspired by nature, numerous techniques have been proposed for fabricating superhydrophobic surfaces using different techniques [9–15].

However, only a few products using such superhydrophobic coating are actually found on the market because of their lack of mechanical stability against abrasion and poor chemical stability. Therefore, it is a highly worthwhile and challenging task to develop a simple, economical, and scalable strategy for fabricating superhydrophobic surfaces with excellent mechanical and chemical durability, with long-term superhydrophobic stability for practical applications.

Aluminum (Al) and its alloys are extensively used in household and a wide range of industrial and household applications. In particular, they are employed in the aerospace, shipping, automotive and construction industries, and in manufacturing household goods because of their high strength, excellent heat and electrical conductivities, and low weight. Corrosion is simply defined as the decay of a metal surface by chemical or electrochemical reactions with its surrounding environment. Because of a thin oxide layer that develops on an Al surface, the surface displays reasonably good corrosion resistance compared to some

✉ Si-Hyung Lim
shlim@kookmin.ac.kr

[1] Nanomechatronics Lab, Kookmin University, Seoul 136-702, South Korea

[2] School of Mechanical Engineering, Kookmin University, Seoul 136-702, South Korea

other metal surfaces. This layer acts as a shield and protects the Al surface from further corrosion. However, Al alloy surfaces having small traces of other metals such as Mn, Fe, Cu, and Mg are more chemically active and therefore prone to corrosion. The susceptibility of an Al alloy surface to corrosion restricts its scope as a potential engineering material for many applications, particularly in wet and salty environments. It is therefore important to improve the corrosion resistance of such surfaces to greatly extend the breadth of its industrial applications. Many methods are used to protect metals against corrosion such as cathodic protection, protective coatings, corrosion inhibitors, and the addition of alloying elements [16–18]. Chrome based coatings is highly effective to protect metal surface from corrosion. However, chromium VI is a toxic substance and carcinogenic to human being and its use in various countries is restricted. Thus, despite their merits, these methods have limitations, including complex, time-consuming, toxic, poor dispersion properties, and adverse effect on the environment.

Thus, compared to conventional methods, there has been a need to develop effective, non-toxic and environmentally friendly corrosion resistance coating or surface inspired by nature. The superhydrophobic coatings with high WCAs represent an important and successful method for preventing damage to the oxide layer on metals and thus protecting the metal surface underneath from further corrosion. For example, the drinking water pipe lines modified with the superhydrophobic coating, not only prevent the surface from corrosion, but also increase the lifespan of the pipe lines and eliminate the health related risks caused by the contaminated water. In recent years, several methods have been reported for preparing a superhydrophobic Al surface with anti-corrosion properties [19–23]. Duan et al. [19] studied the corrosion resistance of the superhydrophobic, layered double hydroxides (LDHs) film on an Al surface. The hierarchical micro-nanostructured superhydrophobic film shows better corrosion resistance than porous anodic alumina film alone or ZnAl-LDH-NO_3^- films. After immersion for 31 days in a 3.5 wt% NaCl solution, the WCA of the ZnAl-LDH-laurate film decreased from 163° to 140°. Similarly, Ou et al. [20] reported the fabrication of a superhydrophobic Al surface via surface roughening with sodium hypochlorite (NaClO), followed by surface passivation by hexadecyltrimethoxysilane. The corrosion current density of the superhydrophobic sample in NaCl solution was much smaller as compared with that of the hydrophilic and hydrophobic one. The WCA of the fabricated surface drastically decreased from 160.8° to 148.1° and the sliding angle increased from 5.5° to 25.2° after immersion in a 3.5 wt% NaCl solution for 7 days. Recently, Zhang et al. [21] demonstrated a one-step electrodeposition approach to fabricate a micro/nano hierarchical papillae superhydrophobic structure on the Al surface in the presence of a mixture of cerium (III) nitrate hexahydrate and hexadecanoic acid electrolytes and investigated their anticorrosion behavior. They reported that the current density of the superhydrophobic surface on Al substrate decreased by more than two orders of magnitude compared to that of the bare Al surface. The result shows a decline in the WCA (a decrease of ~ 5 or 6° from an initial WCA of 167.4°) after exposure to a 3.5 wt% NaCl solution for just 3 days.

However, the use of special equipment and poor long-term durability in corrosive media together with a lack of mechanical stability constrain the uses of superhydrophobic Al surface as anti-corrosion material. Additionally, the usage of expensive fluorine coating may concern environmental issues and limit the practical use of superhydrophobic surfaces. Thus, to extend the application of Al-alloy surfaces, a convenient, inexpensive, and environmentally friendly approach is needed to fabricate Al surface with excellent mechanical, chemical stability, and long-term durability.

In this research, we fabricated the superhydrophobic zinc oxide (ZnO) nanopetals (NPs) on a microstructured (M-structured) Al-alloy substrate (referred as MNP-structured substrate) with high resistance to corrosion and good mechanical stability. This was accomplished by combining three simple processes, namely, a chemical etching and a hydrothermal process, followed by coating with low-surface-energy polydimethylsiloxane (PDMS) using a simple vapor-deposition process (Fig. 1). The Al surface prepared in this way shows superhydrophobicity with a WCA of more than 160° and a WSA of 4°. Chemical etching is a simple and effective method for achieving a rough surface on metals. Zinc oxide with various shape have been widely reported in many literature because of its attractive optical and electrical properties [24–26]. ZnO layer is used as an anti-corrosive coating material and serves as a filler to lengthen the diffusion path of corrosive media. Compared to the other metal oxides, ZnO is cost-effective, and non-toxic material. The deposition of ZnO layer can be easily controlled and hence, it can be applied to the three-dimensional surfaces. Similarly, the PDMS coating is used as a low-surface-energy

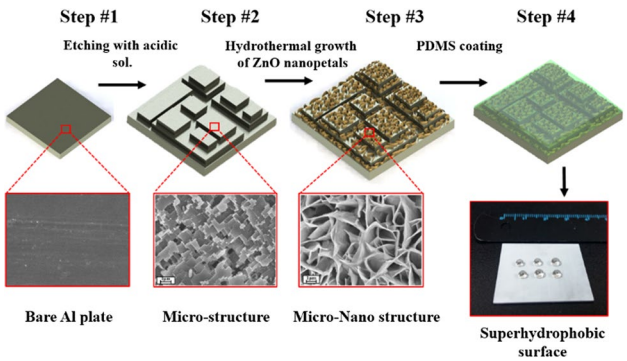

Fig. 1 Schematic diagram of steps involved in fabrication of a superhydrophobic MNP-structure on an Al substrate

material because it is hydrophobic and adhesive nature. Also, PDMS is chemically inert, mechanically flexible, nontoxic, and have minimal environmental impact compared to some other low-surface-energy materials.

The effect of surface morphology on the wettability of the fabricated Al surface has also been investigated. The corrosion behavior of Al surfaces was evaluated using the Tafel polarization technique. The results reveal that the prepared superhydrophobic surface possesses outstanding anti-corrosion properties. Moreover, the chemical stability of the fabricated surface has been explored, and the result shows that the surface is chemically stable against liquids of various pH; this includes long-term exposure to water. More importantly, the superhydrophobic MNP-structured Al surface exhibits good mechanical robustness against the abrasion of sandpaper, along with excellent superhydrophobic properties after storage in an ambient environment for 8 months. The entire process is simple, scalable, and has a variety of prospective applications in industry such as self-cleaning features, water repellency, the corrosion resistance of metals, and oil–water separation.

2 Experimental Section

2.1 Materials

Aluminum alloy plates (6061), hydrochloric acid (HCl), zinc nitrate hexahydrate, hexamethylenetetramine (HMTA), and 1H,1H,2H,2H-perfluorooctyltrichlorosilane (PFOTS) were purchased from Alfa Aesar Inc. The PDMS prepolymer (Sylgard 184A) and curing agent (Sylgard 184B) were purchased from Dow-Corning. The perfluoropolyether (PFPE) (Fomblin®Y, Mw = 2500 g mol^{-1}) and methoxyperfluorobutane (HFE-7100) were purchased from Sigma-Aldrich. All other chemicals were analytical grade and used without further purification.

2.2 Fabrication of dual-scale micro/nanostructures

In the experimental method, an Al plate was cut into small pieces and ultrasonically cleaned in acetone and deionized (DI) water for 3 min each and then dried in a stream of nitrogen. The clean Al plates were then etched with an acidic solution of DI water and HCl (volume ratio 2:1) for 3 min at room temperature to fabricate an M-structured Al substrate. After etching, the samples were washed in DI water and dried in N_2 gas.

The M-structured surface was covered with a film of ZnO NPs using a hydrothermal technique. The substrate was immersed in an aqueous growth solution of zinc nitrate hexahydrate (0.025 M), HMTA (0.025 M), and DI water. After heating at 90 °C for 1 h, the substrate was rinsed with DI water and dried at room temperature. This step created the MNP-structured surface. Finally, the substrate was coated with PDMS layer using a simple vapor-deposition method. In detail, the Al substrate was heated in a beaker containing a PDMS stamp at 230 °C for 1 h. The PDMS stamp was obtained by mixing 1 g of PDMS prepolymer and 0.1 g of a curing agent and then curing at 120 °C for 2 h.

2.3 Characterization

The morphology of the fabricated samples was examined using a field-emission scanning electron microscope (FESEM; JSM-7610 F, JEOL, Japan). The crystal structure of the fabricated samples was examined using an X-ray diffractometer system (XRD) using a Bruker D8 Advance diffractometer with Cu Kα radiation at 40.0 kV and 40.0 mA. The samples were scanned at $2°\theta$ in a range from 30° to 80°. The surface chemical composition of the samples was characterized by X-ray photoelectron spectroscopy (XPS) instrument (K-alpha, Thermo VG, U.K.) using monochromatized Al Kα source working at 12 kV and 3 mA.

The CA and SA were measured for 5 µL droplets of water using a CA measurement system (Phoenix 300 Touch, SEO Co. Ltd, South Korea). The average CA and SA values were obtained by measuring each sample at room temperature at a minimum of five different positions. The CA value was calculated using the tangent line method.

All the electrochemical tests were performed in 3.5 wt% NaCl solution at room temperature using computer-controlled potentiostat (Gamry Instruments Inc, USA) under open circuit conditions. The platinum plate and saturated calomel electrode (SCE) were used as the counter electrode and reference electrode, respectively. All the testing samples were immersed in the NaCl solution for 10 min to ensure the system to be stabilized. The potentiodynamic polarization curves were obtained at a scan rate of 0.33 mV/s from − 0.5 to 1.0 V.

3 Results and Discussion

3.1 Morphology and Chemical Compositions of Fabricated Micro/Nanostructures

Figure 2a shows the top-view SEM images of the M-structured surface obtained by etching method. The entire Al surface was rough and composed of irregular protrusions after etching. The high-resolution images (Fig. 2b, c) confirm that the surface consisted of protuberances that appear similar to building blocks composed of irregularly shaped rectangles. The plateaus were between 1 and 2 µm in size and were consistently distributed over the surface. The mechanism

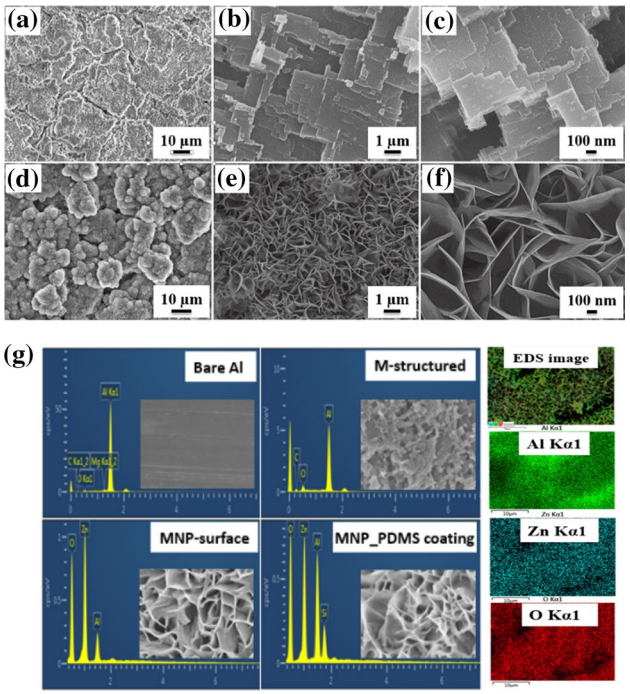

Fig. 2 SEM images of the Al surface **a** M-structured, **d** MNP-structured surface. Images (**b**, **c**) and (**e**, **f**) are high mag. images of (**a**) and (**d**), respectively. Image (**g**) shows the EDS spectra of bare, M-, MNP-structured surface before and after PDMS coating, and chemical element mapping images of ZnO NPs on a M-structured surface

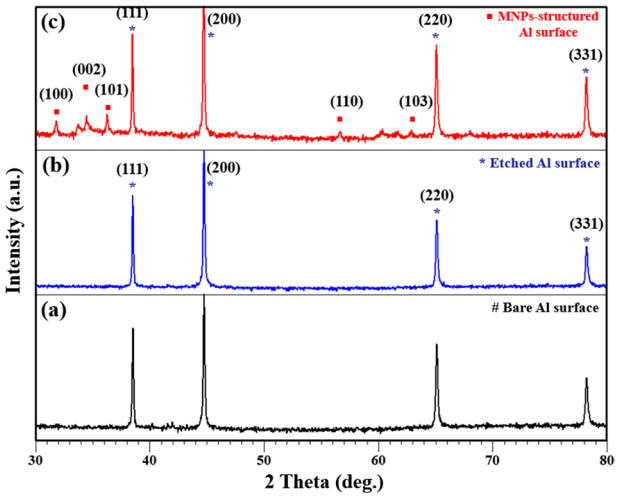

Fig. 3 XRD graph of different Al surfaces **a** bare, **b** etched surface, and **c** MNP-structured Al substrate

for the formation of the microstructure plateaus has been discussed elsewhere [27].

After the hydrothermal treatment, the M-structured substrate was coated with a thin film of ZnO NPs. Figure 2d shows the SEM images of the etched and ZnO-coated Al surfaces obtained after etching and hydrothermal methods. These NPs were predominantly aligned perpendicular to the substrate. The high magnification images in Fig. 2e, f indicate that these NPs exhibited an irregular curved topography with a smooth surface. The images also indicate that the ZnO NPs were self-assembled into a network with an interlocked alignment. The thickness of the NPs was between 20 and 30 nm and they were uniformly assembled onto the microstructure surface of the Al substrate. The surface elemental compositions of the fabricated samples were analyzed using EDS spectroscopy. The EDS spectra and chemical-element mapping images clearly reveal that ZnO NPs were consistently distributed over the M-structured Al surface and after altering the surface with PDMS coating, no significant change in the topography of the MNP-structured substrate was observed, Fig. 2g.

In general, during the hydrothermal growth method, the wurtzite ZnO crystal grows preferentially along the [001] direction due to the lowest surface energy of (002) facet. The growth velocity along <100> direction is slower than that along [001] direction, therefore, 1D ZnO nanorod is often obtained. In our present study, nanopetals-like morphology of ZnO was grown on the M-structured substrate. Al plays an important role in the formation of ZnO NPs. During the hydrothermal reaction, the HMTA reacts with water molecules to produce ammonia and thus provides a controlled supply of OH^- anions. Al is an amphoteric metal and dissolved into the $Al(OH)_4^-$ ions in the presence of alkaline environment of HMTA solution. The additive $Al(OH)_4^-$ ions act as a surface-passivating agent and presumably attach to Zn^{2+} terminated (001) surface. Therefore, the growth of ZnO along [001] direction is suppressed. Hence, the growth proceeds in more than one direction and leads to the formation of ZnO NPs structure [28, 29].

The XRD patterns of the corresponding Al surfaces before and after etching are shown in Fig. 3a, b. The four dominant peaks located at 38.48°,44.72°, 65.08°, and 78.2° correspond to the 111, 200, 220, and 331 diffraction peaks of Al based on the JCPDS data (Card No. 04-0787), indicating that the M-structured rough surface was mainly composed of Al. Figure 3c shows the XRD pattern of the MNP-structured substrate. Five weak diffraction peaks at 31.7°, 34.4°, 36.2°, 56.5°, and 62.8° were detected along with other diffraction peaks attributed to the Al surface. These five peaks can be identified as the hexagonal wurtzite phase of ZnO (JCPDS data No. 76-0704).

We next studied the effect of the hydrothermal processing time on the topography of the ZnO NPs and its consequence for the wetting properties of the fabricated Al surface. The M-structured surface (obtained by etching for 3 min) was immersed in an aqueous solution of 0.025 M $Zn(NO_3)_2{\cdot}6H_2O$ and 0.025 M HMTA and heated at 90 °C for 1, 3, and 5 h. Figure 4 shows the top-view SEM images of the MNP-structured surface in different stages of growth.

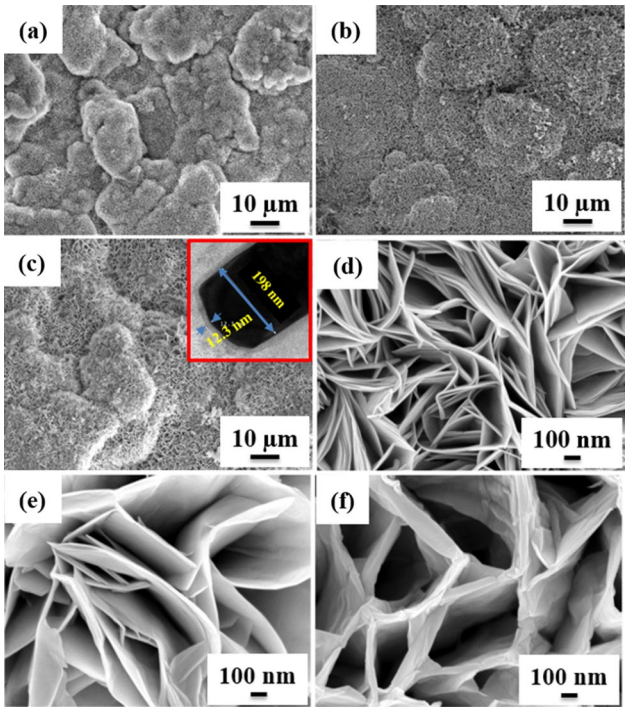

Fig. 4 SEM images of the ZnO NP networks grown on M-structured surfaces after treatment for **a** 1 h, **b** 3 h, and **c** 5 h. Images (**d**), (**e**) and (**f**) are the magnified images of (**a**), (**b**) and (**c**), respectively. Insert shows the TEM image of the PDMS modified ZnO nanostructure

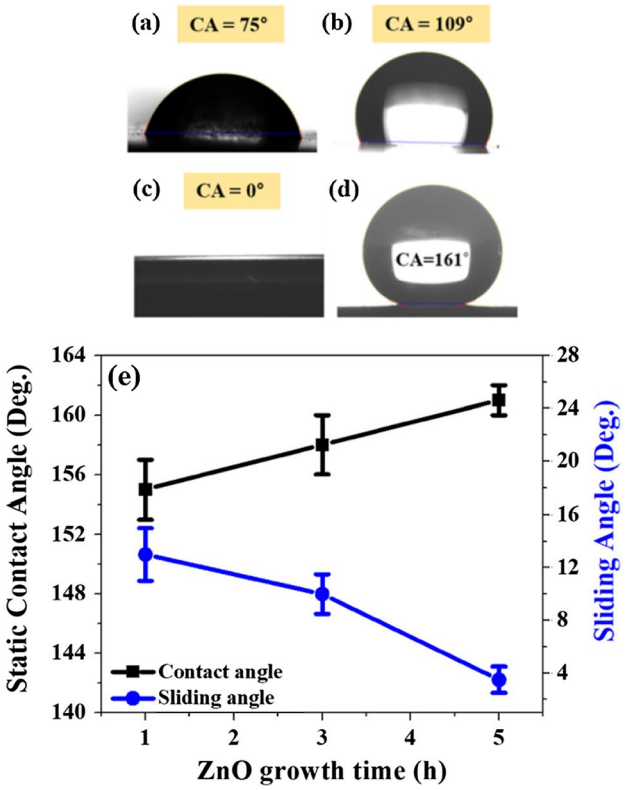

Fig. 5 Images of WCA profile on **a** bare Al, **b** bare surface with PDMS coating, **c** fabricated MNP surface, **d** MNP-structured surface altered with PDMS, and **e** change in the water CAs and SAs of the fabricated surfaces as a function of the hydrothermal growth time

At a reaction time of 1 h, ZnO NPs that self-assembled into clusters can be observed on the M-structured Al surface. The high-magnification image shows that these wrinkles are uniformly distributed over the surface. Upon increasing the reaction time to 3 h, these wrinkles become bigger and they protrude, as shown in Fig. 4b, e. The width of the NPs is thicker and pores can be observed between the self-assembled ZnO NP networks. When the reaction time is increased further to 5 h, the thicker NPs with bigger pore sizes was achieved; the average thickness and the pore diameter of the NPs was 140 nm and 1 µm, respectively. The thickness of the PDMS film was analyzed using transmission electron microscopy (TEM) image, and it can be seen that the surface of ZnO (dark area) is covered by a PDMS film (light color area) with the thickness of about 12.3 nm, Fig. 4c (inset image).

3.2 Surface Wettability

The surface wettability of the prepared Al surface was studied using CA and SA measurements. Figure 5 shows the shapes of water droplets on the different types of Al surfaces. The WCA of the bare Al surface was 75°, indicating hydrophilicity. After PDMS coating, the WCA of the bare surface changed to 113°, indicating hydrophobicity. However, the MNP-structure exhibited superhydrophilicity prior to being coated with PDMS, and the water droplet completely spreading out on the surface to a near-zero contact angle, as shown in Fig. 5c. As mentioned earlier, by controlling two key surface parameters, namely, the surface energy and morphology, superhydrophobic properties can be achieved on a solid surface. Hence, after having been coated with PDMS, the prepared surface changes from superhydrophilic to superhydrophobic (Fig. 5d). The static WCA and the SA of the superhydrophobic surface were found to be 161° and 4°, respectively.

We also examined the surface wettability properties of the fabricated MNP-structured surfaces as a function of the hydrothermal growth time. The surfaces fabricated at different times of 1, 3, and 5 h, after PDMS coating displayed superhydrophobicity with WCAs of 155°, 158°, and 161°, respectively, as shown in Fig. 5e. Thus, the results reveal that after 5 h of hydrothermal growth time, the MNP-structure attained a higher WCA (161°) with a lower WSA of 4°. Because the surface roughness and the pores size between the self-assembled ZnO NP networks increase with increasing the growth time and thus air can be trapped between them (Fig. 4f). This air cushion remarkably decreases the liquid–solid contact area

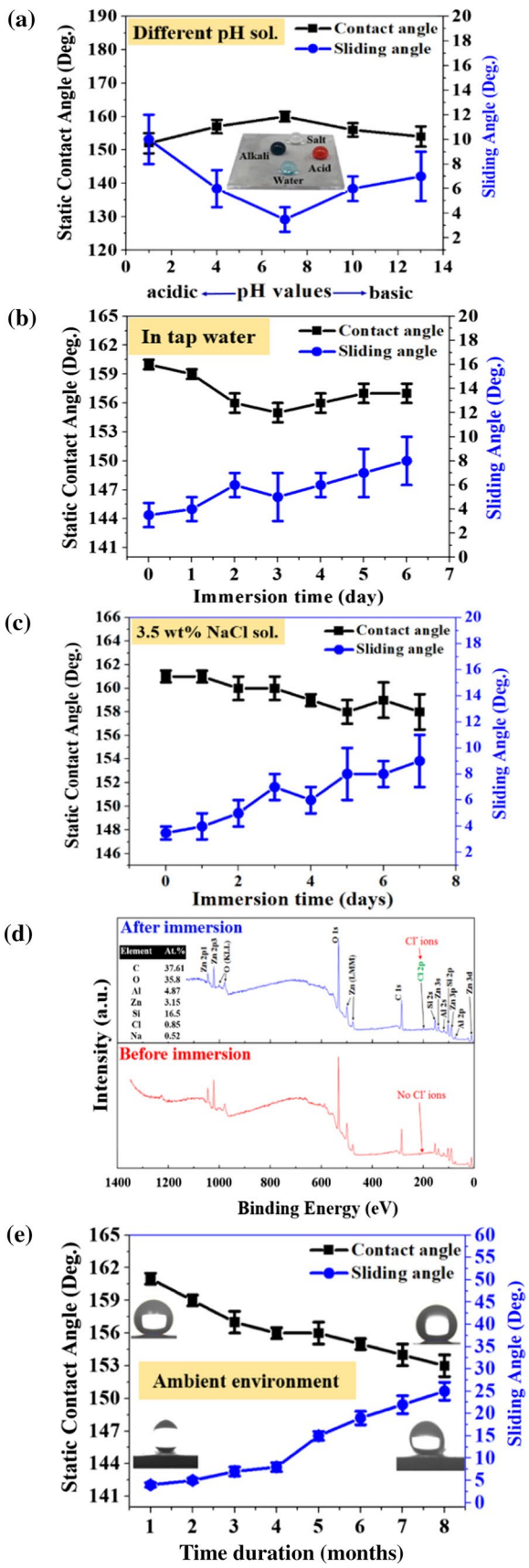

Fig. 6 Variation in the water CAs and SAs of the MNP-structure Al substrate modified with PDMS layer as a function of **a** pH values of water droplets (inset: photograph of liquid droplets with different pH values sitting on the fabricated surface) and **b** immersion time in water, **c** immersion time in the 3.5 wt% NaCl aqueous solution, **d** XPS spectra of the MNP-structure before and after immersion in the 3.5 wt% NaCl aqueous solution for 5 days, and **e** long duration in air at ambient temperature

and thus plays an important role in achieving a higher WCA with better superhydrophobicity.

3.3 Durability of the Superhydrophobic Al Substrate

For the practical application of the superhydrophobic surfaces to become widespread, the surfaces must display high durability. In general, surfaces with high roughness can easily lose their superhydrophobicity when slightly scratched or simply rubbed by human hands; this limits their use in commercial applications. There are a few reports focusing on this aspect of superhydrophobic materials [30–33]. Therefore, in this work, we performed various tests to evaluate the chemical and mechanical stability of the fabricated superhydrophobic surface.

3.4 Chemical Stability

The chemical stability of the fabricated surface was tested under both acidic and basic conditions. Figure 6a shows the relationship between the WCAs and WSAs for the superhydrophobic MNP-surface and solutions with pH values ranging from 1 to 13. The result clearly indicates that the fabricated surface retains its superhydrophobicity with WCAs greater than 150° and SAs less than 10°, revealing that the surface is highly stable in the presence of a corrosive medium.

The WCAs and SAs of the fabricated surface were also examined as a function of the immersion time in the water. As shown in Fig. 6b, marginal variation was observed and the WCA dropped slightly from 160° to 157° after immersion in water for 6 days. However, the WSA remained below 10°, indicating that the fabricated Al surface can maintain its superhydrophobicity with a low sliding angle in water for several days. We also checked the durability of the fabricated surface in a typical corrosive medium, specifically a NaCl solution that is widely used as an aqueous solution to promote a corrosion reaction. Figure 6c displays the variation in the WCAs and SAs of the superhydrophobic MNP-structured surface as a function of immersion time in the 3.5 wt% NaCl solution. The WCA gradually decreased from 161° to 158° and the SAs increased from 4° to 9° with time, but the surface still retained its superhydrophobic characteristic after immersion for 7 days in a highly saline

solution. This slight change in the wettability variation was supposed to be affected by the change in the local chemical property. To confirm this the surface chemical composition of the fabricated Al surface before and after immersion, in 3.5 wt% NaCl solution have been characterized by means of XPS analysis. As shown in Fig. 6d, before immersion in 3.5 wt% NaCl solution, the fabricated surface reveals Al (2p) peak at 76 eV, Al (2 s) peak at 120 eV, and Si (2p) at 102.4 eV from the Al substrate and PDMS coating, respectively. All the other peaks are from ZnO NPs and in good agreement with the standard values of ZnO. After immersion in 3.5 wt% NaCl solution, a very slight peak of Cl element (Cl 2p) appears at 200.6 eV. This clearly indicates that still after immersion in the corrosive medium for 7 days, only a little amount of Cl^- ion existed on the fabricated Al surface and thus it maintained superhydrophobicity.

Furthermore, the superhydrophobic durability of the material is an important factor for extending its practical application in various industries. Hence, the effect of aging was also studied by exposing the fabricated sample at the ambient environment for 8 months. Figure 6e shows a slight decrease in the WCA from 160° to 153° and a water droplet still rolled easily off the surface with a WSA of 22° after 8 months of exposure to air. This clearly implies that the fabricated Al surfaces have excellent long-term stability in air. The slight decline in the CA value for the fabricated surface was possibly due to degradation or damage of the PDMS coating after continued exposure to air.

We also checked the surface morphology of the bare and superhydrophobic surfaces before and after immersion in a 3.5 wt% NaCl solution for 170 h (7 days) using SEM, as illustrated in Fig. 7. After 170 h, the bare Al surface is visibly corroded. The surface was severely damaged and several cracks with associated corrosion products appeared on the surface. In contrast, the superhydrophobic surface did not show any significant change in surface morphology due to immersion. The slight change in the WCA may be due to partial degradation of the PDMS coating because of the attack of the corrosive medium over a long duration. Figure 7e shows the fabricated Al surface immersed in the test solution (3.5 wt% NaCl solution). If viewed at a glancing angle, the superhydrophobic Al surface looks like a silver mirror, indicating that air was trapped in the pores or cavities of the fabricated surface. Thus, such structures are capable of preventing the penetration of liquids into the cavities; and referred to as the Cassie–Baxter state. However, the bare Al substrate was completely wetted with water.

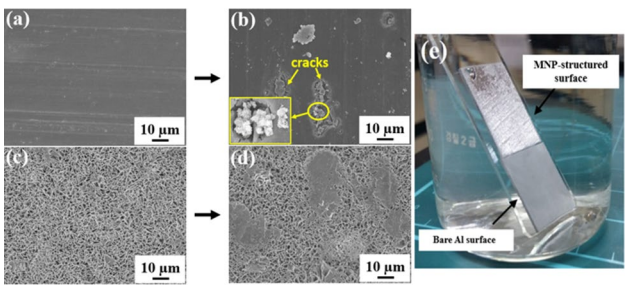

Fig. 7 SEM images of the bare Al surface; **a** before and **b** after immersion in a 3.5 wt% NaCl solution. Superhydrophobic MNP-structured surface **c** before and **d** after immersion in a 3.5 wt% NaCl solution for 7 days. **e** shows the picture of bare and MNP-structured surfaces in a 3.5 wt% NaCl solution

To compare the impact of the PDMS coating on the anti-corrosion properties of the fabricated superhydrophobic surface, we modified the MNP-structured substrates with two other low-surface-energy materials: PFOTS and PFPE. The prepared Al substrate was dipped in a solution of 1% PFOTS in n-hexane for 8 min and then heated on a hot plate at 100 °C for 30 min to achieve superhydrophobicity. Similarly, the other fabricated substrate was immersed in a dilute solution of 1 mM PFPE in HFE-7100 for 18 h and then heated at 150° C for 1 h. As shown in Fig. 8a, all the three fabricated Al substrates displays superhydrophobicity, but among them, the PDMS-coated MNP-structured surface displays the highest WCA (161°) with the lowest SA of 4°.

Finally, all the three samples were immersed in the 3.5 wt% NaCl solution for more than 1 month to examine their long-term resistance performance in the corrosive environment. After immersion for more than 10 days, the WCAs of the PFOTS and PFPE modified Al substrates decreased gradually and then became nearly hydrophilic after 40 days of immersion time, Fig. 8b. The WCAs of the PFOTS- and PFPE-modified Al substrates declined to 76° and 59°, respectively. However, the PDMS-modified MNP-structured substrate retained its superhydrophobicity (152°) even after immersion in the 3.5 wt% NaCl solution for 30 days. The results clearly show that the PDMS-coated Al surface is more resistant to the corrosive medium than are the other coated surfaces. Thus, we can conclude that the MNP-structured surface modified with PDMS is very stable in corrosive medium and has long-term potential for improving the corrosion resistance of the Al substrate. Compared to the recent literature studies, our proposed fabrication technique with superhydrophobic Al surface, provides an effective barrier against corrosive media for a long duration [19–21].

Furthermore, the surface morphology of the fabricated Al substrates was examined using SEM, after having been immersed in a 3.5 wt% NaCl solution for 40 days; this is shown in Fig. 9. The surface morphology of the PDMS modified MNP-structured Al substrates appears to be almost the same as that before immersion, with no substantial change, except some corrosive products appeared on the surface, Fig. 9a, b. However, after immersion for 40 days, PFOTS coating on the fabricated Al surface seems to be completely damaged, Fig. 9c. The high magnification image Fig. 9d,

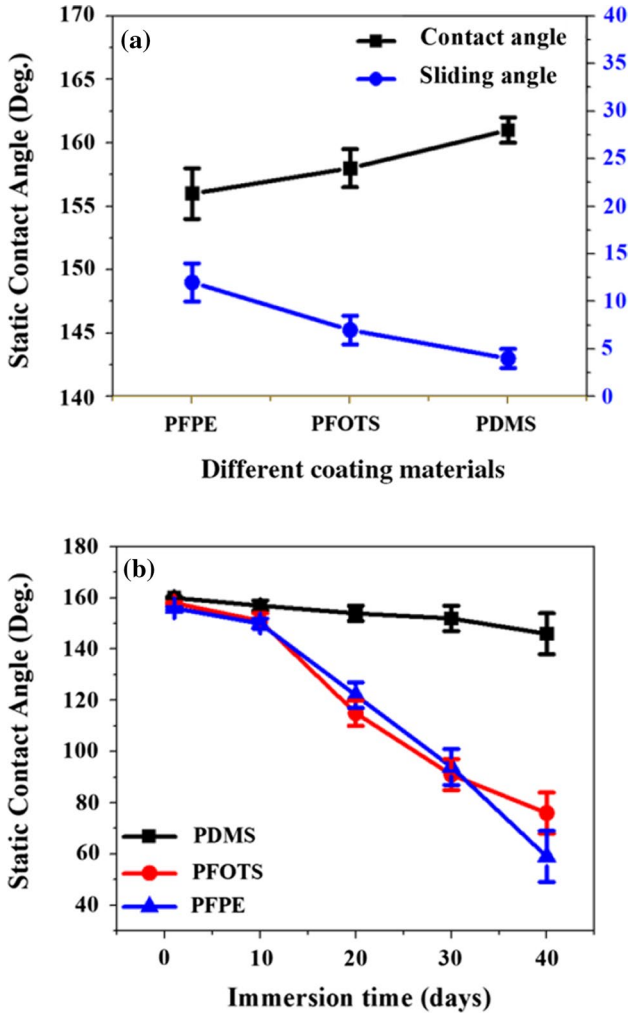

Fig. 8 **a** WCAs and SAs of the fabricated Al surfaces as a function of the different coating materials, **b** change in the WCA measured on the fabricated surfaces modified with different coating materials as a function of the immersion time in the 3.5 wt% NaCl aqueous sol

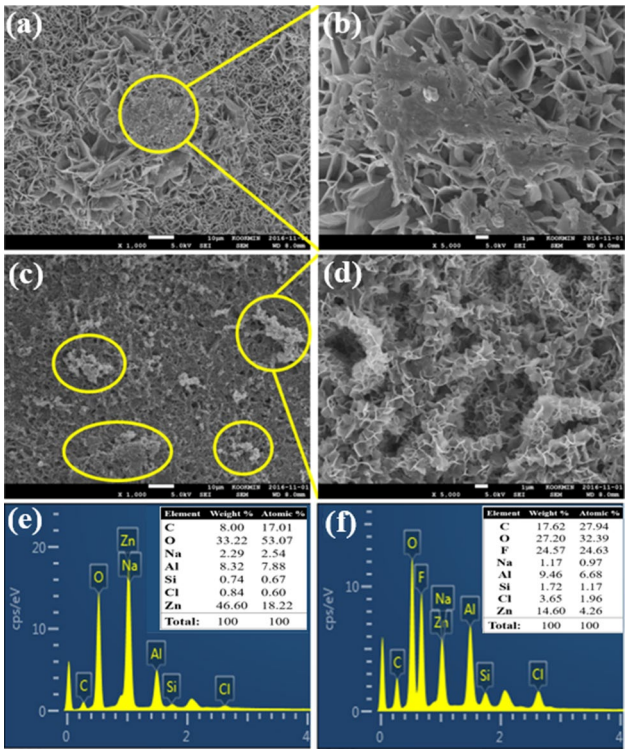

Fig. 9 SEM images of the superhydrophobic MNP-structured substrates **a** with PDMS coating, **c** with PFOTS coating, after immersing in 3.5 wt% NaCl sol. for 40 days. Images (**b**, **e**) and (**d**, **f**) are high mag. images and EDS spectrum of (**a**) and (**b**), respectively

reveals that large number of corrosion products appeared all over the Al surface granular. It indicates with an increase in immersion time, the PFOTS coating gets damaged by the corrosive Cl^- ions and the solution penetrate through the coating and comes in contact with Al alloy surface and the surface persuades to be corroded. The EDS spectrum also clearly confirms the above results, Fig. 9e, f. After 40 days of immersion in 3.5 wt% NaCl solution, the PFOTS coated MNP-structured surface shows higher 3.65 wt% of Cl^- ions on the surface compared to PDMS coating (0.84 wt%).

3.5 Mechanical stability

The mechanical durability of the fabricated surface was investigated via an abrasion test. The abrasion test was carried out using 1000-grit sandpaper as an abrasion surface. The sample to be tested was pressed onto the abrasive material using various pressures. Then the fabricated sample was dragged over the sandpaper at a constant speed in one direction for a length of 60 cm. Figure 10a shows the change in WCA with the increase in pressure applied to the fabricated surfaces. The result indicates that the MNP-structured surface coated with PDMS layer maintained a high WCA (155°) at an applied pressure of 1 kPa. However, an increasing load results in a decrease in the WCA of the fabricated surfaces.

When the applied pressure increases to 5 kPa, the WCA of the fabricated surface decreases to 135°. We believe the PDMS coating on the MNP-structured surface was not sufficiently robust to completely resist the abrasion test at the higher applied pressure, but still maintains its hydrophobic properties.

Furthermore, after the abrasion tests, the morphology of the tested surfaces was examined using SEM imaging. As shown in Fig. 10b, after applying a pressure of 2 kPa, minor scratches were observed on the surface that did not cause severe damage to the MNP-structured surface. The surface appears relatively unchanged with no visible damage. However, as the applied pressure increased to 5 kPa, several scratches were detected on the surface. Figure 10c1 indicates that in a few areas, the surface was damaged and

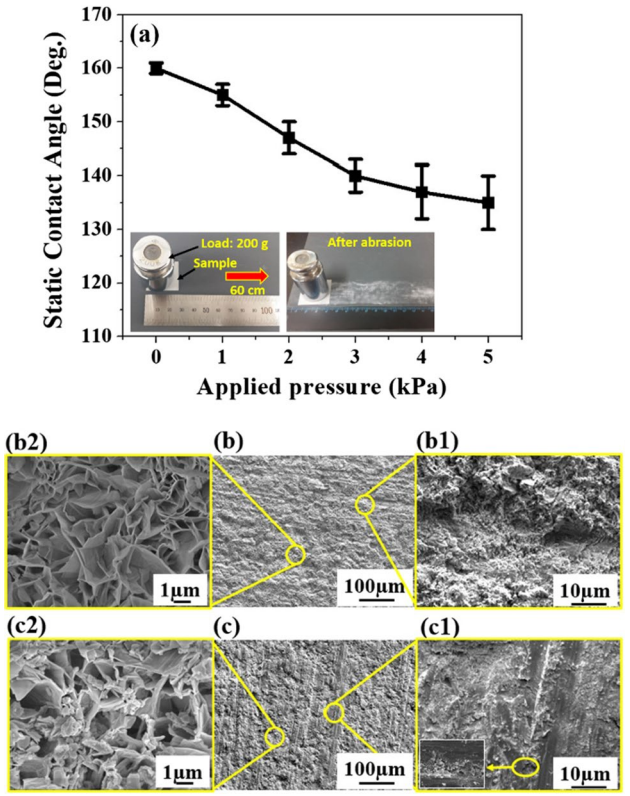

Fig. 10 **a** Variation in the WCA of the superhydrophobic MNP-structured surface after abrasion for 60 cm with increasing applied pressure. SEM images of the corresponding Al surfaces after applying **b** 2 kPa and **c** 5 kPa pressure. The images (b1 and b2) and (c1 and c2) are the high-magnification images of (**b**) and (**c**), respectively

the ZnO nanostructures were completely worn away; however, some lumps of microstructures could still be found on the fabricated surface. The uppermost portions of the ZnO nanostructures appear slightly twisted or compressed, but the microstructures (rectangular shaped plateaus) beneath the top layer nanostructure was well protected and stable. Hence, these microstructures help to retain the hydrophobic properties at the higher applied pressure, as seen in Fig. 10c2.

3.6 Corrosion Resistance Performance

Further, the anti-corrosion performance of the superhydrophobic surface was investigated using an electrochemical corrosion test. The potentiodynamic-polarization curve is a useful method for characterizing the protective behavior of the superhydrophobic surface on the Al substrate. In a typical polarization curve, a higher corrosion potential and a lower corrosion current density correspond to better corrosion resistance and a lower corrosion rate. Figure 11 shows the potentiodynamic-polarization curves of the bare surface, MNP-structure substrate without coating (superhydrophilic)

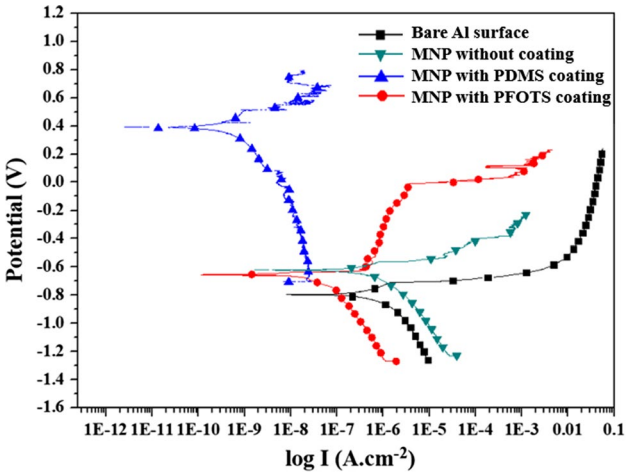

Fig. 11 Potentiodynamic-polarization curves measured in a 3.5 wt% NaCl solution for the bare Al surface, MNP-structured Al surface without any chemical coating, and superhydrophobic MNP-structured Al surfaces modified with PDMS and PFOTS coating

and the surface modified with PDMS and PFOTS coating layers (superhydrophobic) measured in 3.5 wt% NaCl aqueous solution at room temperature. The corrosion parameters such as corrosion current density (i_{corr}) and corrosion potential (E_{corr}) of the samples calculated from the Tafel extrapolation method are shown in Table 1.

It can be seen that the i_{corr} of the superhydrophilic surface (1.653×10^{-7} A cm^{-2}) was slightly lower than that of the bare substrate (3.471×10^{-7} A cm^{-2}), suggesting that the microstructure surface coated with ZnO NPs offers marginally better corrosion protection for the Al substrate. The ZnO NPs act as a passivation layer and elongate the diffusion path of the corrosive medium, along with the protective oxide layer formed on the surface of the Al substrate which acts as barrier helps to improve the corrosion resistance property compared to the bare surface.

The superhydrophobic surfaces has much better corrosion resistance than the bare and the superhydrophilic surface. In the corrosive solution, the corrosion current density of the PDMS-modified superhydrophobic Al surface ($i_{corr}=4.881\times10^{-10}$ A cm^{-2}) is smaller by more than three orders of magnitude than that of the bare and the

Table 1 E_{corr} and i_{corr} for the bare, MNP-structured without coating (superhydrophilic), and the superhydrophobic MNP-structured Al surface after immersion in a 3.5 wt% NaCl solution

Samples	E_{corr} (V)	i_{corr} (A cm^{-2})
Bare	−0.793	3.471×10^{-7}
Superhydrophilic	−0.622	1.653×10^{-7}
Superhydrophobic (PFOTS)	−0.654	7.546×10^{-8}
Superhydrophobic (PDMS)	0.392	4.881×10^{-10}

superhydrophilic surfaces. It is also smaller by two orders of magnitude than that of the superhydrophobic PFOTS-modified Al surface. This indicates the excellent corrosion resistance performance of the PDMS coating. The results also illustrate that the E_{corr} of the PDMS-modified Al substrate (0.392) is more positive than that of the other samples. This further confirms that in a 3.5 wt% NaCl solution, the surface altered with a PDMS coating has better corrosion resistance properties compared to the bare and the PFOTS-modified surfaces.

In the Cassie–Baxter state, on a superhydrophobic surface, air can be easily trapped in the rough surfaces and act as a cushion between the surface and the liquid medium. Therefore, in case of the superhydrophobic Al surface due to its unique surface, a large amount of air was trapped in between the micro/ZnO NPs-structures. This trapped air prevented the infiltration of the corrosive solution into the surface and enhanced the anti-corrosion characteristics of the surface. Finally, the collective effects of the air, the ZnO NP layer and the PDMS coating, which form a triple-layer protective system, also promote better corrosion resistance. However, in the cases of the bare and unmodified MNP-structured Al substrates, the corrosive ions come directly into contact with the surface and easily penetrate it, resulting in the formation of corrosive products accompanied by pits on the surface. The above results clearly verify that both the surface roughness and chemical composition plays a key role in achieving excellent anti-corrosion properties.

Our proposed fabrication method produces excellent anti-corrosion properties on the Al surface compared to those in previously published reports. Liu et al. [34] fabricated a superhydrophobic Al surface using a two-step method involving laser processing and surface modification by n-Dodecyltrimethoxysilane. The superhydrophobic surface displayed a corrosion-current density (i_{corr}) that is smaller by one order of magnitude than that of a bare surface. Similarly, Liang et al. [35] reported that a superhydrophobic hydroxide zinc carbonate film was fabricated on an Al surface using an in situ deposition method and the surface was modified with fluoroalkylsilane molecules. The electrochemical impedance spectroscopy result revealed that the current density of the superhydrophobic Al surface was smaller by more than one order of magnitude compared to that of the bare surface and showed good corrosion resistance. More recently, Chen's group [36] reported an anodization process involving 15 wt% sulfuric acid electrolytes for fabricating a self-cleaning superhydrophobic Al surface (SCSS). The i_{corr} of the SCSS was smaller by three orders of magnitude than that of the bare Al alloy, and the SCSS displayed excellent corrosion resistance. However, in their studies, they did not investigate the anti-corrosion durability of the fabricated Al surface in a typical corrosive medium (NaCl), which we believe is important for scaling up to real industrial applications. Furthermore, as they did not mention mechanical stability, the up-directed structures (such as their fabricated nanowires) are assumed to be fragile and could be easily damaged when subjected to high levels of applied force.

It is well known that the corrosion of the surface is affected by the defects. In the scratched or damaged surfaces, the corrosive ions easily penetrate through these defects and directly comes in contact with surface. Therefore, we also investigated the corrosion resistance property of the mechanically damaged MNP-structured substrate coated with PDMS layer. The abrasion test was carried out on the MNP-structured Al substrate, similarly as described earlier with an applied pressure of 5 kPa. The electrochemical corrosion tests was performed on the MNP-structured Al substrate coated with PDMS layer after the scratch in 3.5 wt% NaCl solution, to examine the corrosion resistance property of the damaged surface. The result indicates that the corrosion current density of the PDMS modified MNP-structured Al substrate after scratching ($i_{corr} = 7.458 \times 10^{-8}$ A cm^{-2}) is higher than that of the PDMS modified MNP-structured Al substrate before scratching ($i_{corr} = 4.881 \times 10^{-10}$ A cm^{-2}). The shift of the corrosion current density in the higher direction, clearly indicates that the ZnO nanostructures including PDMS coating get damaged. However, even after the abrasion at the applied pressure of 5 kPa, the scratched Al substrate shows better corrosion resistance property compared to the bare Al surface ($i_{corr} = 3.471 \times 10^{-7}$ A cm^{-2}). We also checked the corrosion resistance performance of the scratched MNP-structured Al substrate after repeating the vapor-deposition of PDMS. The corrosion current density of the damage repaired Al substrate ($i_{corr} = 5.854 \times 10^{-9}$ A cm^{-2}) decreased by two orders of magnitude and one order of magnitude as compared to the bare Al substrate and the scratched MNP-structured Al substrate, respectively.

4 Conclusions

Superhydrophobic coatings were successfully fabricated on an Al alloy surface by means of chemical etching combined with a hydrothermal method, followed by coating with PDMS via a simple vapor deposition technique. The fabrication process resulted in a water CA greater than 160° and an SA less than 5°. The superhydrophobicity of the fabricated Al surface derives from a rough surface characterized by microstructured rectangular plateaus combined with a self-assembled network of ZnO nanopetals. In addition to superhydrophobicity, the fabricated surface exhibits excellent chemical stability under both harsh acidic and alkaline environments. The anti-corrosion properties of the fabricated Al surfaces covered with different low-surface-energy coating materials were investigated using

potentiodynamic-polarization curves and the result revealed that the PDMS-modified superhydrophobic surface shows high resistance to corrosion, more than three orders of magnitude greater than that of other surfaces. The PDMS-modified MNP-structured Al substrate retained superhydrophobicity after being immersed in a 3.5 wt% NaCl for more than 1 month. Thus, we can conclude that, compared to other low-surface-energy materials, our proposed PDMS-coating technique is very effective in enhancing the long-term corrosion resistance of the fabricated Al surface. Due to the special micro- and nanostructured surface, the superhydrophobic surface shows good mechanical durability with long-term stability in an ambient environment. After 8 months of exposure to air, the fabricated Al surface displays superhydrophobicity with a WCA of 153° and a sliding angle of 22°. Thus, we believe this simple fabrication process combined with its advantageous properties makes it an ideal candidate for the production of a scalable, three-dimensional superhydrophobic material suitable for many industrial applications.

Acknowledgements This research was supported by the National Research Foundation (NRF) funded by the Ministry of Science, Republic of Korea (Grant number: 2016R1A2B3015530).

References

1. Yao, X., Song, Y. L., & Jiang, L. (2011). Applications of bio-inspired special wettable surfaces. *Advanced Materials, 23*(6), 719–734.
2. Blossey, R. (2003). Self-cleaning surfaces-virtual realities. *Nature Materials, 2,* 301–306.
3. Boinovich, L. B., Emelyanenko, A. M., Ivanov, V. K., & Pashinin, A. S. (2013). Durable icephobic coating for stainless steel. *ACS Applied Materials & Interfaces, 5*(7), 2549–2554.
4. Jung, Y., Jung, K. K., Park, B. G., & Ko, J. S. (2018). Capacitive oil detector using hydrophobic and oleophilic PDMS sponge. *International Journal of Precision Engineering and Manufacturing, 5*(2), 303–309.
5. Liu, H. Q., Szunerits, S., Xu, W. G., & Boukherroub, R. (2009). Preparation of superhydrophobic coatings on zinc as effective corrosion barriers. *ACS Applied Materials & Interfaces, 1,* 1150–1153.
6. Zheng, S., Li, C., Fu, Q., Hu, W., Xiang, T., Wang, Q., et al. (2016). Development of stable superhydrophobic coatings on aluminum surface for corrosion-resistant, self-cleaning, and anti-icing applications. *Materials and Design, 93,* 261–270.
7. Lee, C., & Kim, C. (2011). Underwater restoration and retention of gases on superhydrophobic surfaces for drag reduction. *Journal of Physical Review Letters, 106,* 0145021–0145024.
8. Kobayashi, M., Terayama, Y., Yamaguchi, H., Terada, M., Murakami, D., Ishihara, K., et al. (2012). Wettability and antifouling behavior on the surfaces of superhydrophilic polymer brushes. *Langmuir, 28,* 7212–7222.
9. Kwon, Y., Patanker, N., Choi, J., & Lee, J. (2009). Design of surface hierarchy for extreme hydrophobicity. *Langmuir, 25,* 6129–6136.
10. Xu, L., Karunakaran, R. G., Guo, J., & Yang, S. (2012). Transparent, superhydrophobic surfaces from one-step spin coating of hydrophobic nanoparticles. *ACS Applied Materials & Interfaces, 4*(2), 1118–1125.
11. Wu, X., Fu, Q., Kumar, D., Ho, J. W. C., Kanhere, P., Zhou, H., et al. (2016). Mechanically robust superhydrophobic and superoleophobic coatings derived by sol–gel method. *Materials and Design, 89,* 1302–1309.
12. Ko, H., Yi, H., & Jeong, H. E. (2017). Wall and Ceiling Climbing Quadruped Robot with Superior Water Repellency Manufactured Using 3D Printing (UNIclimb). *International Journal of Precision Engineering and Manufacturing, 4*(3), 273–280.
13. Zhu, Y., Zhang, J. C., Zheng, Y. M., Huang, Z. B., Feng, L., & Jiang, L. (2006). Superhydrophobic, and conductive polyaniline/polystyrene films for corrosive environments. *Advanced Functional Materials, 16,* 568–574.
14. Xu, W., Song, J., Sun, J., Lu, Y., & Yu, Z. (2011). Rapid fabrication of large-area, corrosion-resistant superhydrophobic Mg alloy surfaces. *Applied Materials & Interfaces, 3,* 4404–4414.
15. Lee, S. H., Lee, J. H., Park, C. W., Lee, C. Y., Kim, K., et al. (2014). Continuous fabrication of bio-inspired water collecting surface via roll-type photolithography. *International Journal of Precision Engineering and Manufacturing, 1*(2), 119–124.
16. Guo, W. X., Li, X. Y., Chen, M. X., Xu, L., Dong, L., Cao, X., et al. (2014). Electrochemical cathodic protection powered by triboelectric nanogenerator. *Advanced Functional Materials, 24,* 6691–6699.
17. Deshpande, P. P., Jadhav, N. G., Gelling, V. J., & Sazou, D. (2014). Conducting polymers for corrosion protection: a review. *Journal of Coatings Technology and Research, 11,* 473–494.
18. Gandel, D. S., Easton, M. A., Gibson, M. A., Abbott, T., & Birbilis, N. (2014). The influence of zirconium additions on the corrosion of magnesium. *Corrosion Science, 81,* 27–35.
19. Zhang, F., Zhao, L., Chen, H., Xu, S., Evans, D. G., & Duan, X. (2008). Corrosion resistance of superhydrophobic layered double hydroxide films on aluminum. *Angewandte Chemie International Edition, 47,* 2466–2469.
20. Lv, D., Ou, J., Xue, M., & Wang, F. (2015). Stability and corrosion resistance of superhydrophobic surface on oxidized aluminum in NaCl aqueous solution. *Applied Surface Science, 333,* 163–169.
21. Zhang, B., Zhao, X., Li, Y., & Hou, B. (2016). Fabrication of durable anticorrosion superhydrophobic surfaces on aluminum substrates via a facile one-step electrodeposition approach. *RSC Advance, 6,* 35455–35465.
22. Boinovich, L. B., Emelyanenko, A. M., Modestov, A. D., Domantovsky, A. G., & Emelyanenko, K. A. (2015). Synergistic effect of superhydrophobicity and oxidized layers on corrosion resistance of aluminum alloy surface textured by nanosecond laser treatment. *ACS Applied Materials & Interfaces, 7,* 19500–19508.
23. Yin, Y., Liu, T., Chen, S., Liu, T., & Cheng, S. (2008). Structure stability and corrosion inhibition of superhydrophobic film on aluminum in seawater. *Applied Surface Science, 255,* 2978–2984.
24. Suh, Y. D., Hong, S. J., Kim, G. H., Hwang, K. I., Choi, J. H., et al. (2016). Selective electro-thermal growth of zinc oxide nanowire on photolithographically patterned electrode for microsensor applications. *International Journal of Precision Engineering and Manufacturing, 3*(2), 173–177.
25. Gurav, A. B., Latthe, S. S., Vhatkar, R. S., Lee, J. G., Kim, D. Y., Park, J. J., et al. (2014). Superhydrophobic surface decorated with vertical ZnO nanorods modified by stearic acid. *Ceramics International, 40,* 7151–7160.
26. Yeo, J., Kim, G., Hong, S., Lee, J., Kwon, J., Lee, H., et al. (2014). "Single nanowire resistive nano-heater for highly localized thermo-chemical reactions: localized hierarchical heterojunction nanowire growth. *Small, 10*(24), 5015–5022.
27. Qian, B. T., & Shen, Z. Q. (2005). Fabrication of superhydrophobic surfaces by dislocation-selective chemical etching on aluminum, copper, and zinc substrates. *Langmuir, 21,* 9007–9009.

28. Cheng, J. P., Zhang, X. B., & Luo, Z. Q. (2008). Oriented growth of ZnO nanostructures on Si and Al substrates. *Surface & Coatings Technology, 202,* 4681–4686.
29. Liu, J., Xu, L., Wei, B., Lv, W., Gao, H., & Zhang, X. (2011). One-step hydrothermal synthesis and optical properties of aluminium doped ZnO hexagonal nanoplates on a zinc substrate. *CrystEngComm, 13,* 1283–1286.
30. Zhu, X. T., Zhang, Z. Z., Yang, J., Xu, X. H., Men, X. H., & Zhou, X. Y. (2012). "Facile fabrication of a superhydrophobic fabric with mechanical stability and easy-repairability. *Journal of Colloid Interface and Science, 380,* 182–186.
31. Lee, S. M., Kim, K. S., Pippel, E., Kim, S., Kim, J. H., & Lee, H. J. (2012). Facile route toward mechanically stable superhydrophobic copper using oxidation_reduction induced morphology changes. *Journal of Physical Chemistry C, 116,* 2781–2790.
32. Guo, F., Su, X. J., Hou, G. L., & Li, P. (2012). Bioinspired fabrication of stable and robust superhydrophobic steel surface with hierarchical flowerlike structure. *Colloid Surface A, 401,* 61–67.
33. Maitra, T., Antonini, C., Mauer, M. A., Stamatopoulos, C., Tiwari, M. K., & Poulikakos, D. (2014). Hierarchically nanotextured surfaces maintaining superhydrophobicity under severely adverse conditions. *Nanoscale, 6,* 8710–8719.
34. Liu, Y., Liu, J., Li, S., Han, Z., Yu, S., & Ren, L. (2014). Fabrication of biomimetic super-hydrophobic surface on aluminum alloy. *Journal of Materials Science, 49,* 1624–1629.
35. Liang, J., Hu, Y., Wu, Y., & Chen, H. (2013). Fabrication and corrosion resistance of superhydrophobic hydroxide zinc carbonate film on aluminum substrates. *Journal of Nanomaterials, 2013,* 139768 (6 pages).
36. Zheng, S., Li, C., Fu, Q., Li, M., Hu, W., Wang, Q., et al. (2015). Fabrication of self-cleaning superhydrophobic surface on aluminium alloys with excellent corrosion resistance. *Surface & Coatings Technology, 276,* 341–348.

Publisher's Note Springer Nature remains neutral with regard to jurisdictional claims in published maps and institutional affiliations.

Sumit Barthwal received his Ph.D. degree in the field of chemistry from Kookmin University, South Korea in 2016 under the supervision of Professor Si-Hyung Lim. At present he is working as research professor in Nano Mechatronics Lab, Kookmin University. His research interests focus on the fabrication of the bioinspired superhydrophobic and superoleophobic surfaces including fabrication of anti-icing and anti-corrosion surfaces.

Si-Hyung Lim received his B.S. and M.S. degrees in School of Mechanical and Aerospace Engineering at Seoul National University, Seoul, Korea, in 1994 and 1996, respectively, and his Ph.D. degree in Department of Mechanical Engineering at UC, Berkeley, CA, USA, in 2005. He is currently a Full Professor in School of Mechanical Engineering at Kookmin University, Seoul, Korea. His current research interests include biomimetic functional surface patterning and MEMS sensors & actuators.